Histol Histopathol (2012) 27: 1029-1040
DOI: 10.14670/HH-27.1029

http://www.hh.um.es

Histology and Histopathology
Cellular and Molecular Biology

Trehalose treatment accelerates the healing of UVB-irradiated corneas. Comparative immunohistochemical studies on corneal cryostat sections and corneal impression cytology

Jitka Čejková[1], Čestmír Čejka[1] and Jacques Luyckx[2]

[1]Laboratory of Eye Histochemistry and Pharmacology, Institute of Experimental Medicine, Center of Excellence, Academy of Sciences of the Czech Republic, Prague, Czech Republic and [2]Laboratoires Thea, Clermont-Ferrand, France

Summary. The UVB-irradiated cornea is damaged by oxidative stress. Toxic oxygen products induced by UVB radiation in the cornea are insufficiently removed by antioxidants, whose numbers decrease with increasing UVB irradiation. In addition, the UVB-irradiated cornea suffers from hypoxic conditions because damaged corneal cells cannot utilize oxygen normally, although the supply of oxygen to the cornea is unchanged (normal). This contributes to attenuated re-epithelialization, corneal neovascularization and apoptotic cell death. Our previous publications reported that trehalose applied on the corneal surface during irradiation significantly suppressed UVB-induced corneal oxidative damage. The results of this study provide for the first time important evidence that trehalose applied on the surface of corneas for two weeks following repeated UVB irradiation (312 nm, daily dose 0.5 J/cm^2) accelerated corneal healing, restored corneal transparency and suppressed corneal neovascularization. Compared to buffered saline treatment, following which caspase-3, nitrotyrosine, malondialdehyde and urokinase-type plasminogen activator were still strongly expressed in the corneal epithelium two weeks after irradiation and corneal neovascularization was evident, apoptotic cell death was already significantly reduced after one week of trehalose application. The expression of other markers of injury returned to normal levels during two weeks of trehalose treatment.

In conclusion, our results show that trehalose accelerated healing of the UVB irradiated cornea, very probably via suppression of hypoxia-response injury. In addition, immunohistochemical results on corneal cryostat sections corresponded with those obtained using corneal impression cytologies, thus confirming that corneal impression cytologies are useful for diagnostic purposes.

Key words: Trehalose, UVB rays, Corneal healing

Offprint requests to: Prof. Jitka Čejková, MD, PhD, DSc, Head, Department of Eye Histochemistry and Pharmacology, Institute of Experimental Medicine, Academy of Sciences of the Czech Republic Vídeňská 1083, 14220, Prague 4, Czech Republic. e-mail: cejkova@biomed.cas.cz

Introduction

Trehalose, a disaccharide of glucose, has been shown to be effective in protecting cells against a variety of stressful environmental conditions, such as dessication, dehydration, heat, cold, oxidation and hypoxia or even anoxia (Elbein et al., 2003; Chen and Haddad, 2004; Minutoli et al., 2007; Chen et al., 2009; Jain and Roy, 2009; Luyckx and Baudouin, 2011). Tissue injury due to oxidative stress is present in many ocular diseases and injuries, including UVB radiation, which induce the generation of reactive oxygen species (e.g. Wenk et al., 2001). The cornea absorbs and detoxifies the majority of UVB rays reaching the eye; however, under circumstances when a threshold amount of UVB rays is exceeded (e.g., due to the thinned ozone layer and the more pronounced penetration of solar UVB radiation), a series of harmful disturbances appear, such as changes in corneal optics (Cejka et al., 2007), morphological disorders of the corneal epithelium (Koliopoulus and Margaritis, 1979; Haaskjold et al., 1993; Podskochy 2000; Rogers et al., 2004), activation of the plasminogen activator/plasmin system (Čejková and Lojda, 1995), alterations in corneal metabolites (Tessem et al., 2005; Fris et al., 2006), the induction of

reactive oxygen and nitrogen species (Čejková et al., 2005), proinflammatory cytokine expression and corneal neovascularization (Pauloin et al., 2009; Čejková et al., 2011). UVB radiation causes a decrease in antioxidants in the cornea, whereas prooxidants remain at normal levels or even increase, leading to the development of an antioxidant/prooxidant imbalance (Čejková et al., 2004). Trehalose dropped on the ocular surface during UVB irradiation reduced pro-inflammatory cytokine induction, decreased metalloproteinase and xanthine oxidase expression and reduced the antioxidant/prooxidant imbalance in the corneal epithelium (Čejková et al., 2011). Nitric oxide synthases, which generate nitric oxide, were largely suppressed in the cornea after trehalose treatment and the formation of cytotoxic peroxynitrite was decreased. Corneal neovascularization was also markedly suppressed (Čejková et al., 2010). Because trehalose effectively protected the rabbit cornea against the damaging effect of UVB radiation if applied during the irradiation procedure, we decided to examine in this study the effect of trehalose on the healing properties of the cornea already damaged by repeated UVB radiation. Rabbit corneas were repeatedly irradiated with UVB radiation (312 nm, daily dose of 0.5 J/cm^2) for four days, then trehalose (or buffered saline) was dropped on the corneal surface (six times daily) during the subsequent three weeks. After sacrificing the animals, immunohistochemistry was employed to detect active caspase-3, nitrotyrosine, malondialdehyde and urokinase-type plasminogen activator on cryostat sections of the cornea, and the results were compared with those obtained on corneal impression cytologies collected during the healing process. Corneal healing was also evaluated morphologically and macroscopically (photographic documentation).

UVB radiation (312 nm, daily dose of 0.5 J/cm^2), employed in this study and also previously (Čejková et al., 2010, 2011) for the irradiation of the rabbit cornea, is equivalent approximately to 5 hrs exposure time of the human cornea to UVB rays from sunlight (according to Zigman, 1995). This corresponds to the recent measurements of Sasaki (2009).

Materials and methods

Adult female New Zealand white rabbits (2.5-3.0 kg) were used in our experiments. The investigation was conducted according to the ARVO Statement on the Use of Animals in Ophthalmic and Vision Research. Rabbits (twelve animals were employed and the whole experiment was repeated once) were anesthetized by an intramuscular injection of Rometar (Xylazinum hydrochloricum, Spofa, Prague, CR, 2%, 0.2 ml/kg body weight) and Narkamon (Ketaminum hydro-chloricum, Spofa, 5%, 1 ml/kg body weight). The open eyes of anesthetized rabbits were irradiated (both eyes of each rabbit) with a UVB lamp (Bioblock Scientific, Illkirch Cedex, France; 312 nm wavelength, 6W) with a dose of 0.5 J/cm^2 per day for four days. The daily irradiation took place from a distance of 0.06 m for 5 min. A UV lamp stand - with an exactly determined distance between the lamp and the eye of the animal - was employed for irradiation. The plane of the lamp was parallel to the tangential plane of the eye (perpendicular to the optical axis of the eye). The intensity of irradiation was regularly measured with a UVB sensor connected to a radiometer (both instruments manufactured by Cole-Parmer Inc., Vernon Hills, Illinois, USA). The total dose of irradiation was also checked using these devices. Although the source of UVB that was used emits only UVB rays peaking at 312 nm (according to the irradiation spectrum given by the manufacturer), a UVC sensor (Cole-Parmer Inc.) was employed to check for the potential emission of UVC light. During irradiation, the eyes of anesthetized animals were held open. Only the cornea was irradiated, the rest of the ocular surface was protected by means of a device made of sterile gauze (slighty soaked with aqua pro injectione for softening) with the central hole of the same diameter as the rabbit cornea.

After finishing the irradiation procedures (day four of repeated irradiation), three animals were sacrificed under i.v. injection of thiopental anesthesia (Thiopental, Spofa, 30 mg/kg following premedication with intramuscular injection of Rometar/Narkamon) and the excised corneas were employed for immunohistochemical examinations. The other animals were treated (by dropping three drops in each eye, six times daily) with trehalose (right eye) or buffered saline (left eye) for one week (three animals), two weeks (three animals) and three weeks (three animals).

After the end of treatment the animals were sacrificed and the corneas microscopically examined. Normal corneas from untreated animals served as controls. During the whole experiment the eyes were photographically documented and corneal impression cytologies collected (at the end of the irradiation procedures and following one, two and three weeks of treatment with trehalose or buffered saline).

Ophthalmic solutions

Trehalose (87.6mM) preservative-free eye drops (Thealoz®) were supplied by Laboratoires Thea, Clermont-Ferrand, France. Trehalose (anhydrous) was dissolved in an aqueous vehicle containing sodium chloride in order to adjust the tonicity (315 mosml/kg) and Tris buffer (pH 7.4). Phosphate-buffered saline (0.01 M) was used as the negative control.

Preparation of cryostat sections, immunohistochemical and morphological examinations

After sacrificing the animals the eyes were enucleated and the anterior eye segments dissected out and quenched in light petroleum chilled with an acetone-dry ice mixture. Sections were cut on a cryostat and transferred to glass slides.

Subsequently, the cryostat sections were fixed in acetone at 4°C for 5 min. For the immunohistochemical localization of peroxynitrite (by nitrotyrosine residues), active caspase-3, malondialdehyde and urokinase-type plasminogen activator, the following primary antibodies were used: monoclonal mouse anti-nitrotyrosine (Abcam, Cambridge, UK), monoclonal mouse anti-human caspase 3 (Abcam, Cambridge, UK), polyclonal goat anti-malondialdehyde (US Biological, Swampscott, MA, USA), monoclonal mouse anti- urokinase-type plasminogen activator Ab-1 (Neomarkers, Fremont, CA, USA). The binding of the primary antibodies was demonstrated using the HRP/DAB Ultra Vision Detection System (Thermo Scientific, Fremont, CA, USA) following the instructions of the manufacturer: hydrogen peroxide block (15 min), ultra V block (5 min), primary antibody incubation (60 min) (mouse monoclonal anti-tyrosine 1 μg/ml, mouse anti-human caspase 2 μg/ml, monoclonal mouse anti-urokinase type plasminogen activator 2 μg/ml, polyclonal (0.5 μg/ml) (Santa Cruz Biotechnology, Santa Cruz, CA, USA) secondary antibody incubation (10 min) and peroxidase-labeled streptavidin incubation (10 min). Visualization was performed using freshly prepared DAB substrate-chromogen solution.

Cryostat sections in which the primary antibodies were omitted from the incubation media served as negative controls. Some sections were counterstained with Mayer's hematoxylin.

Corneal impression cytologies, sample collection, immunohistochemical examination

Corneal epithelial cells were obtained using Millicell membranes (Millicell-CM, hydrophylic PTFE, Millipore Corporation, Billerica, MA 01821, USA) as described previously for conjunctival epithelial cells (Čejková et al. 2008). Briefly: First, 0.4% oxybuprocaine hydrochloride (single drop) was instilled to the eye. (Corneal impression cytologies were also collected in sleeping intramuscularly anesthetized animals). To remove superficial corneal epithelial cells, strips of Millicell membrane were gently pressed for 5 seconds onto the corneal surface. The specimens (corneal cells on the Millicells) were stored at -80°C until they were employed for immunohistochemical examination. The Millicell membranes with corneal epithelial cells were fixed in acetone for 1 minute, released from the plastic holder, rinsed with PBS (phosphate buffered saline tablets, Sigma), placed cell side up on round 12 mm coverslips and then (after rinsing with PBS) permeabilised with 0.2% triton (Triton X 100, Sigma) in PBS. Similar primary and secondary antibodies were employed for the detection of active caspase-3, nitrotyrosine, malondialdehyde and urokinase-type plasminogen activator as described for immunohistochemistry with cryostat sections. Negative controls included the omission of the primary antibody. Some samples were counterstained with Mayers' hematoxylin (Sigma). After the staining procedure, the samples were immediately examined using an Orthoplan Leitz light microscope equipped with a Leica DC 500 digital camera.

Statistics

Mann-Whitney U test was used to investigate the differences between groups: the UVB-irradiated corneas treated with trehalose vs. normal untreated corneas or UVB-irradiated corneas treated with buffered saline drops vs. normal untreated corneas. The number of caspase-3 positive cells in the corneal epithelium, as well as the number of corneal epithelial cells positively stained for malondialdehyde, nitrotyrosine and urokinase type plasminogen activator were counted (central as well as limbal corneal regions) over an area 100 μm long and 100 μm wide in sagittal cryostat sections or Millicell membranes.

Results

The healing of UVB-irradiated corneas following one and two weeks of trehalose or buffered saline treatment (Figs. 1-4).

Immunohistochemical detection of active caspase-3

In the corneas irradiated four times with UVB, pronounced staining for active caspase-3 was found in the corneal epithelium (Fig. 1a,b). After one week of buffered saline treatment, active caspase-3 remained strongly expressed in the corneal epithelial cells (Fig. 1 c,d). In contrast, following one week of trehalose application, only rare apoptotic cells (arrows) were present in the corneal epithelium (Fig. 1e,f). After two weeks of buffered saline treatment, active caspase-3 was still strongly expressed in the superficial epithelial layers (arrows) (Fig. 1g,h), whereas after two weeks of trehalose treatment, no apoptotic cells were present in the corneal epithelium (Fig. 1i,j). The staining was very similar as in the normal corneal epithelium (Fig. 1k,l). In cryostat sections as well as corneal impression cytologies in which the primary antibody was omitted from the incubation medium, no positive staining appeared (Fig. 1m,n). In Fig. 1, the cryostat sections, as well as the corneal impression cytology samples were counterstained with haematoxylin.

Immunohistochemical detection of nitrotyrosine

Nitrotyrosine staining was pronounced in the corneal epithelium of the corneas irradiated with UVB rays (Fig. 2a,b). Following one week of buffered saline treatment, nitrotyrosine staining remained pronounced in the corneal epithelium (Fig. 2c,d). In contrast, following one week of trehalose application, nitrotyrosine staining was

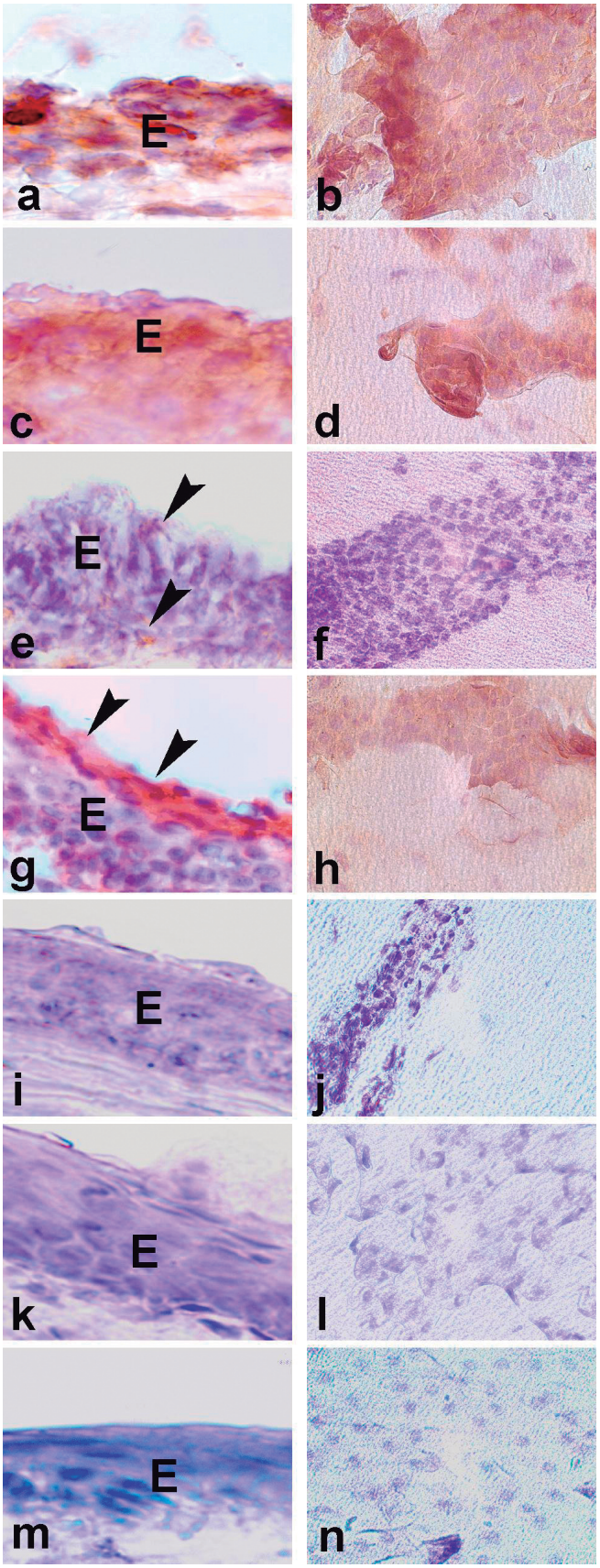

reduced in the irradiated epithelium (Fig. 2e,f). Following two weeks of buffered saline treatment, nitrotyrosine staining was still present in the corneal epithelium (Fig. 2g,h), whereas after two weeks of trehalose application no nitrotyrosine staining was observed in the corneal epithelium (Fig. 2i,j). The staining was very similar to the normal corneal epithelium (Fig. 2k,l) where nitrotyrosine staining was absent. In the negative controls, in which the primary antibody was omitted from the incubation medium, no positive staining appeared (Fig. 2m,n). In Fig. 2 the cryostat sections as well as the corneal impression cytology samples were counterstained with haematoxylin.

Immunohistochemical detection of malondialdehyde

In the UVB-irradiated corneal epithelium, strong staining for malondialdehyde was evident in the corneal epithelium (Fig. 3a,b). Following one week of buffered saline treatment, malondialdehyde staining remained pronounced in the epithelium (Fig. 3c,d), whereas after trehalose eye drops malondialdehyde staining was reduced in the corneal epithelial cells (Fig. 3e,f). After two weeks of buffered saline treatment, malondialdehyde staining was still present in the corneal epithelium (Fig. 3g,h). In contrast, following two weeks of trehalose treatment, malondialdehyde staining was absent in the corneal epithelium (Fig. 3i,j), very similar to the normal corneal epithelium (Fig. 3k,l). Fig. 3m, n: no positive staining appeared in the negative controls (primary antibody omitted from the incubation medium). In Fig. 3 the cryostat sections as well as the corneal cytology samples were counterstained with haematoxylin.

Fig. 1. Staining for active caspase-3 (counterstained with haematoxylin). Cryostat sections: Fig. 1 (**a, c, e, g, i, k, m)** (E - corneal epithelium); corneal impression cytologies: Fig. 1 (**b, d, f, h, j, l, n)**. **a, b.** Cornea irradiated four times with UVB radiation. Strong caspase-3 expression is seen in the corneal epithelium (**a** - cryostat section, **b** - impression cytology sample). **c, d.** Irradiated cornea treated with buffered saline for one week after the end of irradiation. Caspase-3 staining is prominent in the corneal epithelium (c - cryostat section, **d** - impression cytology sample). **e, f.** Irradiated cornea treated with trehalose eye drops for one week after the end of irradiation. Only rare apoptotic cells are present in the corneal epithelium (arrows) (**e** - cryostat section, **f** - impression cytology sample). **g, h.** Irradiated cornea treated with buffered saline for two weeks after the end of irradiation. Active caspase-3 is present in the superficial epithelial layers (arrows) (**g** - cryostat section, **h** - impression cytology sample). **i, j.** Irradiated cornea on which trehalose drops were applied for two weeks after irradiation. No positive staining for active caspase-3 is seen in the corneal epithelium (**i** - cryostat section, **j** - impression cytology). **k, l.** Normal cornea. Positive staining for active caspase-3 is absent in the corneal epithelial cells (**k** - cryostat section, **l** - impression cytology). **m, n.** Control section (m), control impression cytology sample (n). No positive staining appears (primary antibody was omitted from the incubation medium). Scale bar: 10 μm.

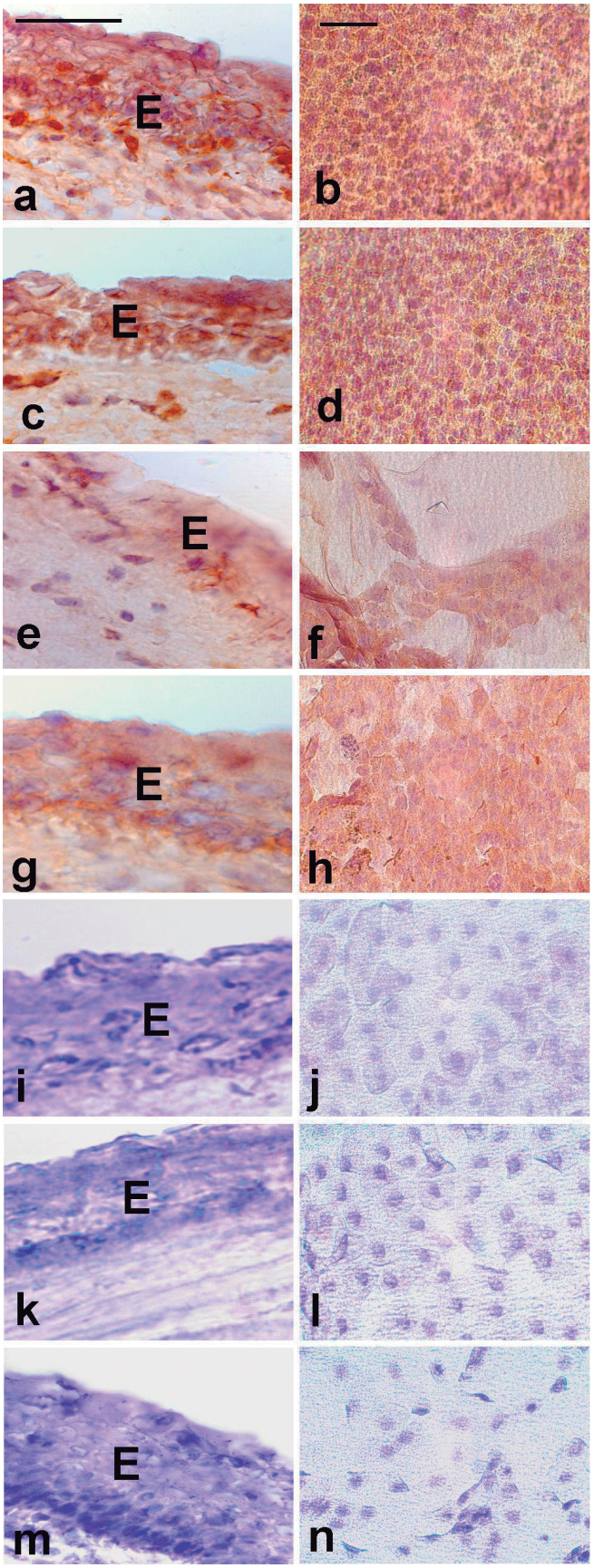

Immunohistochemical detection of urokinase-type plasminogen activator

After four days of repeated irradiation with UVB rays, there was markedly pronounced staining for urokinase-type plasminogen activator in the corneal epithelium (Fig. 4a,b). Following one week of buffered saline treatment, urokinase-type plasminogen activator expression remained pronounced in the corneal epithelium (Fig. 4c,d), whereas after one week of trehalose drops the expression of the enzyme was reduced in the irradiated corneal epithelium (Fig. 4e,f). After two weeks of buffered saline treatment the enzyme expression remained high in the corneal epithelium (Fig. 4g,h). In contrast, following two weeks of trehalose drops enzyme expression was low in the corneal epithelium (Fig. 4i,j), very similar as in the normal corneal epithelium (Fig. 4k,l). Negative control: no positive staining appeared when the primary antibody was omitted from the incubation medium (Fig. 4m,n). In Fig. 4 the cryostat sections as well as the corneal cytology samples were counterstained with haematoxylin.

The healing of UVB-irradiated corneas following three weeks of buffered saline treatment (Table 1).

After the end of the third week of buffered saline application on UVB irradiated cornea many apoptotic cells were found in the corneal epithelium, and corneal epithelial cells revealed the staining for nitrotyrosine and malondialdehyde, as well as urokinase type plasminogen activator (findings on cryostat sections as well as corneal impression cytologies). This was in contrast to the

Fig. 2. The staining of nitrotyrosine (counterstained with haematoxylin). Corneal cryostat sections: Fig. 2 (**a, c, e, g, i, k, m**) (E - corneal epithelium). Corneal impression cytologies: Fig. 2 (**b, d, f, h, j, l, n**). **a, b.** The expression of nitrotyrosine in corneal epithelium irradiated four times with UVB rays. Nitrotyrosine staining is clearly visible in the corneal epithelium (**a** - cryostat section, **b** - impression cytology sample). **c, d.** Irradiated cornea treated with buffered saline for one week after irradiation. The staining for nitrotyrosine is highly pronounced in the corneal epithelium (**c** - cryostat section, d - impression cytology sample). **e, f.** Irradiated cornea treated with trehalose for one week after the last irradiation procedure. Low levels of nitrotyrosine are present in the epithelium (**e** - cryostat section, f - impression cytology sample). **g, h.** Irradiated cornea on which buffered saline was applied for two weeks after the last irradiation. Nitrotyrosine staining is present in the corneal epithelium (g - cryostat section, h - impression cytology sample). **i, j.** Irradiated cornea treated with trehalose drops for two weeks after the end of the irradiation procedure. No positive staining is seen in the cornea (i - cryostat section, j - impression cytology sample). **k, l.** Normal cornea. Nitrotyrosine staining is absent in the corneal epithelium. The epithelium is counterstained only (**k** - cryostat section, **l** - impression cytology sample). **m, n.** Control section (m), control impression cytology sample (n). No positive staining appears when the primary antibody is omitted from the incubation medium. Scale bar: 10 μM.

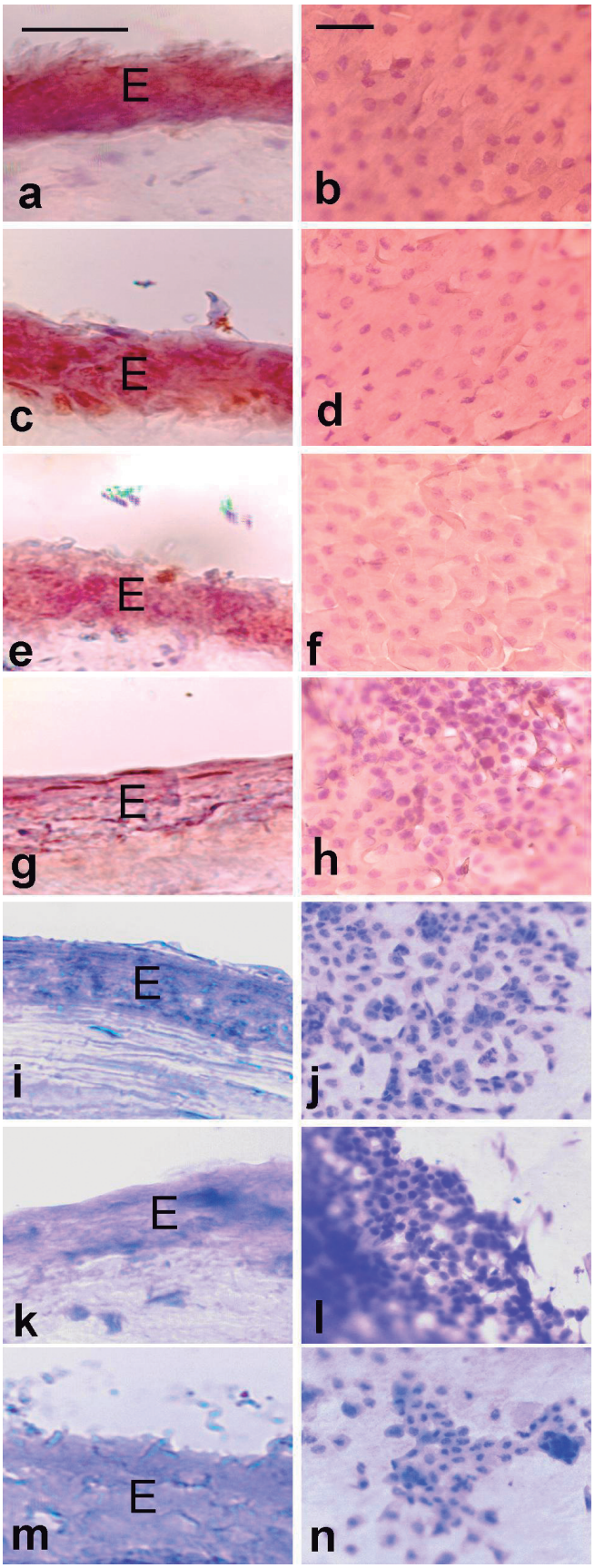

trehalose-treated UVB-irradiated corneas, where following two weeks of treatment the immunohistochemical staining of corneal epithelial cells for active caspase-3, nitrotyrosine, malondialdehyde and urokinase-type plasminogen activator was similar to the normal untreated cornea: in the corneal epithelium only isolated apoptotic cells were present. The expression of urokinase type plasminogen activator was very low in the corneal epithelium and the staining of nitrotyrosine and malondialdehyde was absent. Cryostat sections as well as samples on Millicell membranes were stained only by counterstaining.

Macroscopical evaluation of UVB-irradiated corneas treated with buffered saline or trehalose, Fig. 5

After the last irradiation, corneal transparency was lost and the corneas were highly vascularized (white arrows) (Fig. 5b, the eye before buffered saline treatment, Fig. 5c, the eye before trehalose treatment, white arrows point to neovascularization) - compare with the normal cornea (Fig. 5a). After one week of buffered saline application, the irradiated corneas were opaque and profoundly vascularized (white arrows). The central corneal region was not re-epithelialized (black arrow) (Fig. 5d). Following trehalose treatment for one week, corneal transparency was restored (black arrow); however, marked corneal neovascularization was seen at the limbal region (white arrows) (Fig. 5e). After two weeks of buffered saline application on the UVB-irradiated corneas the alterations of the corneal epithelium (lost superficial epithelial layers) were not healed in the corneal centers (black arrow), which is easily seen in the transparent corneas, and corneal neovascularization was highly pronounced (white arrows) (Fig. 5f). In contrast, after two weeks of

Fig. 3. Malondialdehyde staining (counterstained with haematoxylin). Corneal cryostat sections: Fig. 3 (**a, c, e, g, i, k, m**) (E – corneal epithelium); corneal impression cytologies: Fig. 3 (**b, d, f, h, j, l, n**). **a, b.** Cornea irradiated with UVB radiation for four days. Malondialdehyde staining is strong in the corneal epithelium (a - cryostat section, **b.** Impression cytology sample) **c, d.** Irradiated cornea treated for one week with buffered saline. Malondialdehyde staining is stll strong in the corneal epithelium (**c** - cryostat section, d - impression cytology sample). **e, f.** Irradiated cornea on which trehalose was dropped for one week after the last irradiation. The staining for malondialdehyde is less pronounced. Compare with buffered saline treatment (c - cryostat section, **d** - impression cytology sample). **g, h.** Cornea treated with buffered saline for two weeks after irradiation. Malondialdehyde staining is present in the corneal epithelium (**g** - cryostat section, h - impression cytology sample). **i, j.** Cornea treated with trehalose for two weeks following irradiation. Malondialdehyde staining is absent in the corneal epithelium (**i** - cryostat section, j - impression cytology sample). **k, l.** Normal cornea. Malondialdehyde staining is not present in the corneal epithelium (**k** - cryostat section, l - impression cytology sample). **m, n.** Negative control. The primary antibody was omitted from the incubation medium. No positive staining is present in the epithelium (**m** - cryostat section, **n** - impression cytology sample). Scale bar: 10 μm.

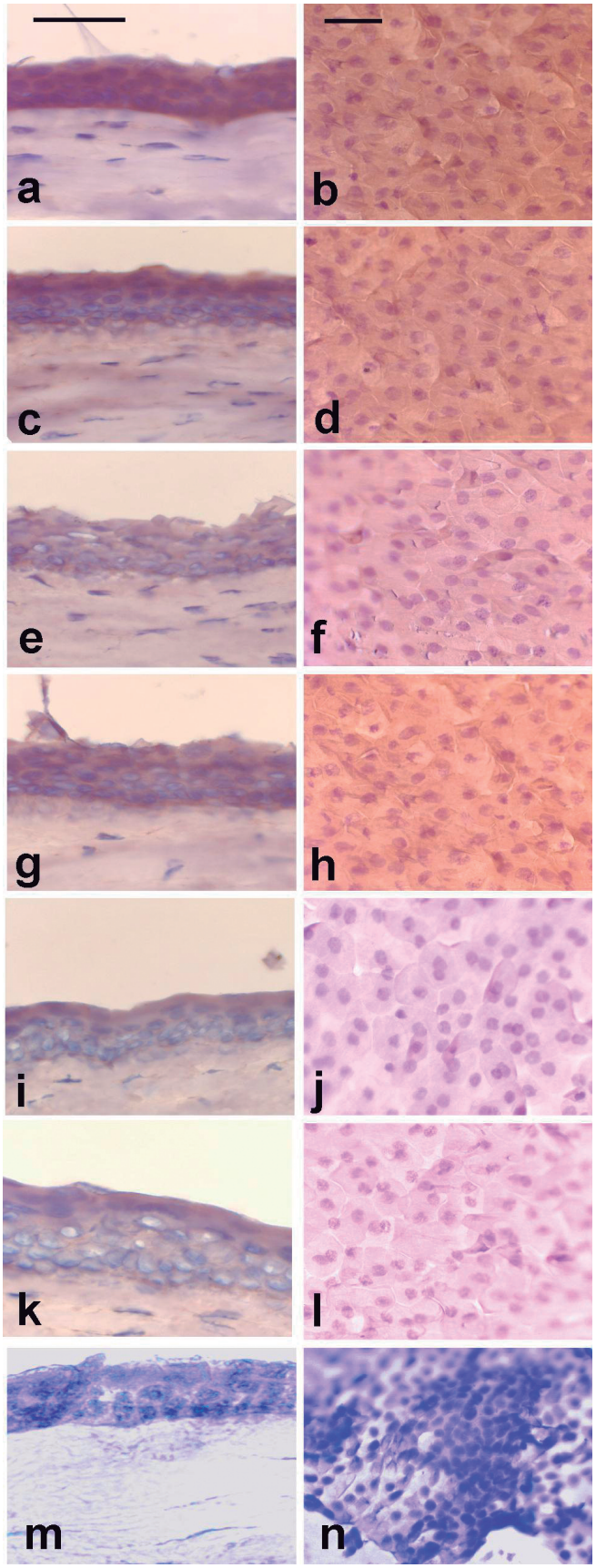

trehalose application the corneas were re-epithelialized (black arrow) and neovascularization was reduced (white arrows) (Fig. 5g). After three weeks of buffered saline application the corneas were not re-epithelialized in the central region (black arrow) and remained markedly vascularized (white arrows) (Fig. 5h), whereas following three weeks of trehalose drops corneal neovascularization was suppressed (white arrows) in the re-epithelialized corneas (black arrow) (Fig. 5i).

Morphological demonstration of corneal healing following buffered saline or trehalose treatment (E - epithelium) (Fig. 6).

After two weeks of buffered saline treatment of the UVB-irradiated cornea the corneal epithelium was thinner in the central region (superficial layers of the corneal epithelium were lacking) (arrow) (Fig. 6a), whereas following two weeks of trehalose drops, the cornea was re-epithelialized (arrow) (Fig. 6b). Normal cornea (Fig. 6c).

Corneal neovascularization in detail (Fig. 7).

After three weeks of buffered saline treatment, neovascularization of the cornea was apparent (black arrows) (Fig. 7a), whereas following trehalose application corneal neovascularization was suppressed (black arrows) (Fig. 7b). Compare to a normal eye (Fig. 7c) without initial vascularization (black arrows).

Statistics

Statistical results for UVB-irradiated corneal epithelium (vs. normal, untreated corneal epithelium)

Fig. 4. Urokinase-type plasminogen activator (counterstained with haematoxylin). Corneal cryostat sections: **Fig. 4** (**a, c, e, g, i, k, m**) (E - corneal epithelium); corneal impression cytologies: Fig. 4 (**b, d, f, h, j, l, n**). **a, b.** A cornea irradiated four times with UVB rays. Pronounced staining for the enzyme is apparent in the corneal epithelium (**a** - cryostat section, **b** - impression cytology sample). **c, d.** Cornea treated with buffered saline for one week after irradiation. Staining for the enzyme is strong in the corneal epithelium (**c** - cryostat section, **d** - impression cytology sample). **e, f.** Cornea on which trehalose drops were applied for one week after irradiation. The enzyme expression is reduced in the corneal epithelium (**e** - cryostat section, **f** - impression cytology sample). **g, h.** Cornea treated with buffered saline for two weeks following irradiation procedure. The staining remains high in the corneal epithelium (**g** - cryostat section, **h** - impression cytology sample). **i, j.** Cornea on which trehalose was applied for two weeks after the last irradiation procedure. The enzyme expression is low in the corneal epithelium, very similar to that seen in the normal corneal epithelium (more staining in the superficial layers) (**i** - cryostat section, **j** - impression cytology sample). **k, l.** Normal cornea. The staining is low in the corneal epithelium (stronger in the superficial layers) (**k** - cryostat section, **l** - impression cytology sample). **m, n.** Negative control. The primary antibody was omitted from the incubation medium (**m** - cryostat section, **n** - impression cytology sample). No positive staining appears. Scale bar: 10 μm.

treated with trehalose drops or buffered saline drops from day 0 (four times irradiated rabbit cornea with the daily dose of 0.5 J/cm^2) to day 21 is shown in Table 1. The number of positively stained cells was decreasing along with the prolonged time interval after the irradiation: very quickly after the treatment with trehalose drops and very slowly after buffered saline drops.

Discussion

Trehalose, a disaccharide of glucose stored in many organisms, although not in mammals, is synthesized as a stress response factor when cells are exposed to stressful conditions. The accumulation of trehalose in cells was found to be associated with increased tolerance against heat, dehydration, oxidation, hypoxia and even anoxia

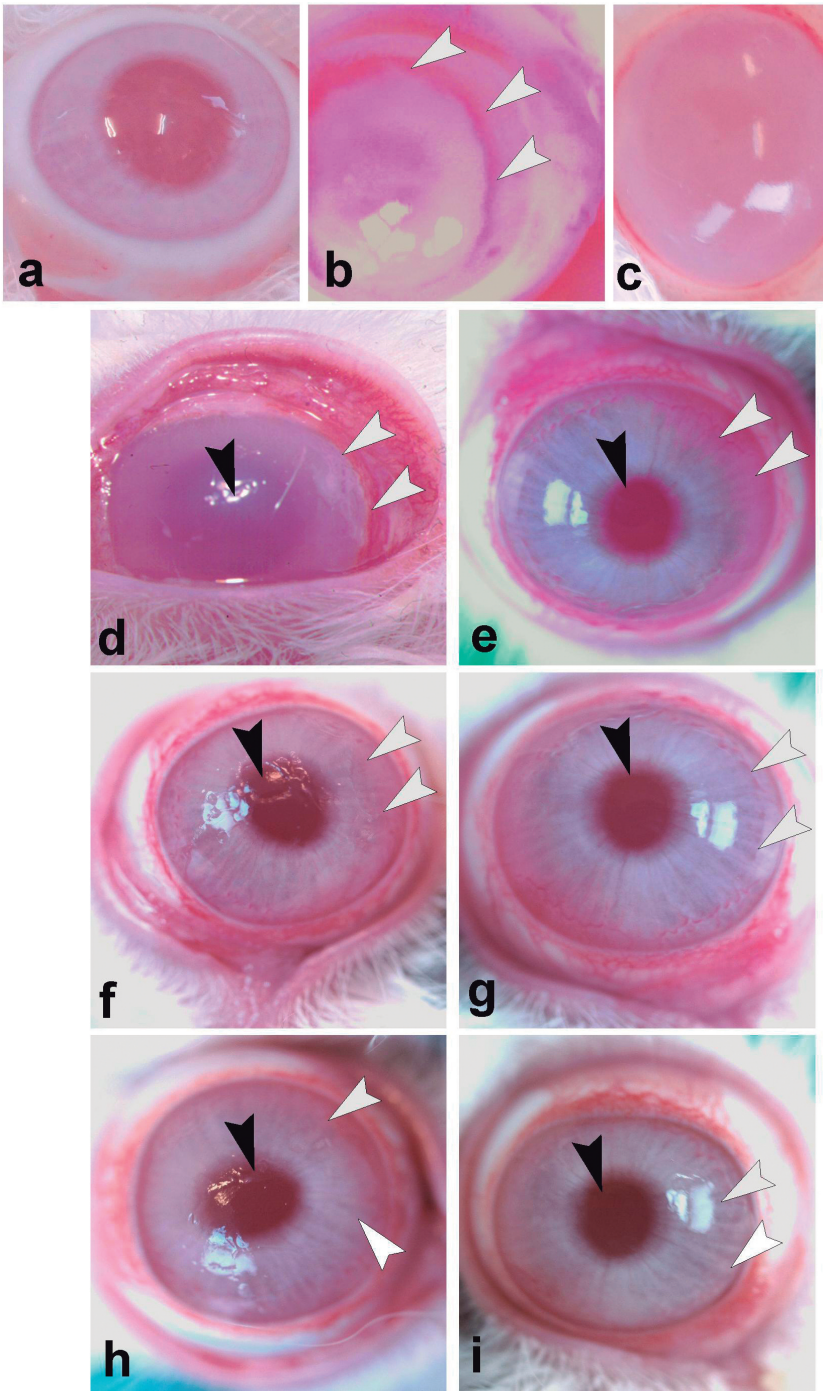

Fig. 5. Macroscopic images of the healing of UVB-irradiated corneas. **a.** Normal cornea. **b.** Cornea irradiated four times with a dose of 0.5 J/cm2 of UVB radiation. The transparency of the cornea is lost and the cornea is profoundly vascularized (white arrows). (The eye before the treatment with buffered saline drops). **c.** Very similar picture of the cornea as in **b**. (The eye before the treatment with trehalose drops). **d.** A cornea treated with buffered saline for one week after irradiation. The cornea is opaque with the central epithelial lesion (black arrow) and neovascularization is highly pronounced (white arrows). **e.** Irradiated cornea treated with trehalose for one week after irradiation. Corneal transparency is restored (black arrow); however, corneal neovascularization is highly pronounced in the limbal region (white arrows). **f.** UVB-irradiated cornea after two weeks of buffered saline treatment. The cornea is not completely re-epithelialized in the central corneal region (black arrow), which is well seen in the transparent cornea, and neovascularization of the cornea is highly pronounced (white arrows). **g.** UVB-irradiated cornea treated for two weeks with trehalose drops. The cornea is re-epithelialized (black arrow) and neovascularization of the cornea is reduced (white arrows). **h.** UVB-irradiated cornea on which buffered saline was applied for three weeks. Central corneal epithelial defects are not completely healed (black arrow) and neovascularization of the cornea is pronounced in the limbal region (white arrows). **i.** UVB-irradiated cornea treated with trehalose drops for three weeks after UVB irradiation. Corneal neovascularization is suppressed (white arrows) in the re-epithelialized cornea (black arrow).

Table 1. UVB-irradiated corneal epithelium treated with trehalose or buffered saline drops vs. normal (untreated) corneal epithelium.

Day of trehalose treatment	Caspase	NT	MDA	U-PA	Day of saline treatment	Caspase	NT	MDA	U-PA
Day 0	h.s.	h.s.	h.s.	h.s.	Day 0	h.s.	h.s.	h.s.	h.s.
Day 7	s.	h.s.	h.s.	s.	Day 7	h.s.	h.s.	h.s.	h.s.
Day 14	n.s.	n.s.	n.s.	n.s.	Day 14	h.s.	h.s.	h.s.	h.s.
Day 21	n.s.	n.s.	n.s.	n.s.	Day 21	s.	h.s.	h.s.	s.

Normal (untreated) corneal epithelium

Caspase	NT	MDA	U-PA
solely corneal epithelial cells stained (solely apoptosis)	no positive staining of corneal epithelial cells	no positive staining of corneal epithelial cells	very low staining of corneal ep. cells

Mann-Whitney U test was used for statistical evaluation of differences between groups: UVB-irradiated corneal epithelium vs. normal corneal epithelium (untreated corneas) in the number of positive cells for active caspase-3, malondiladehyde, nitrotyrosine and plasminogen activator of urokinase type stainings in various time intervals ofthe treatment with trehalose or buffered saline drops. h.s., significant $p<0.01$; s., significant $p<0.05$; n.s., not significant; Caspase, active caspase-3 staining; NT, nitrotyrosine staining; MDA, malondialdehyde staining; UPA, urokinase type plasminogen activator staining.

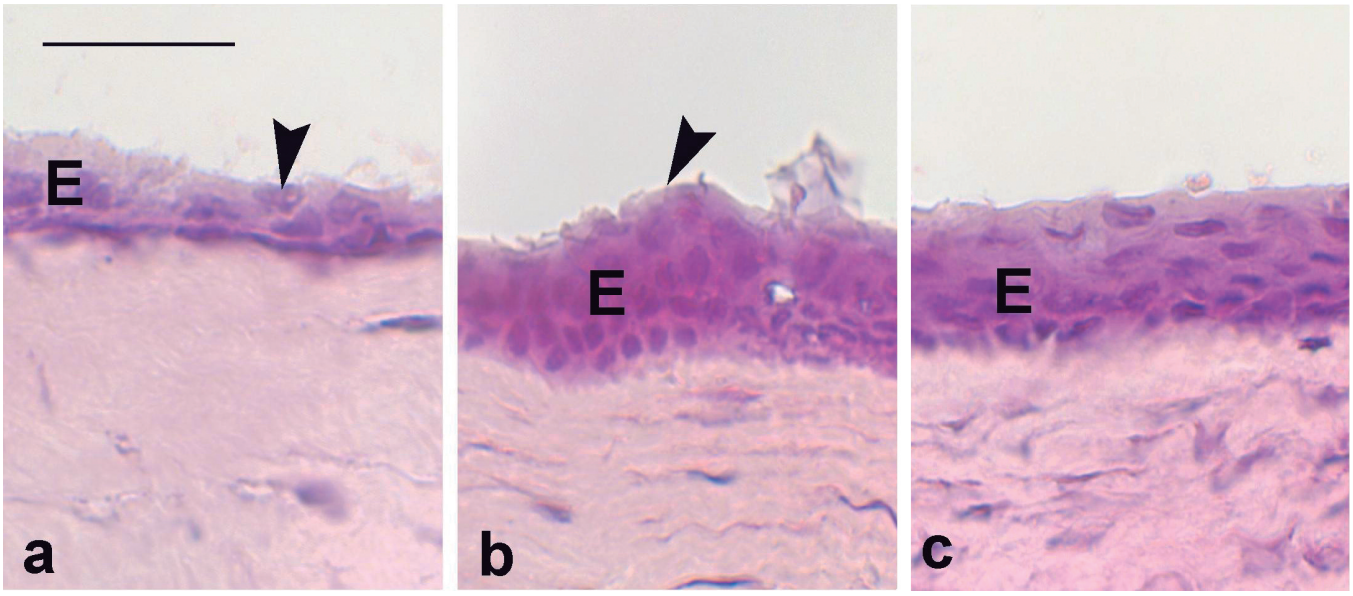

Fig. 6. Morphological picture of the healing of UVB-irradiated corneas (haematoxylin-eosin staining). (E - epithelium). **a.** Irradiated cornea after two weeks of buffered saline treatment. In the central part of the cornea the superficial epithelial layers are missing (arrow). **b.** Irradiated cornea on which trehalose drops were applied for two weeks after irradiation. The cornea is re-epithelialized (arrow). **c.** Normal cornea. Scale bar: 10 μm.

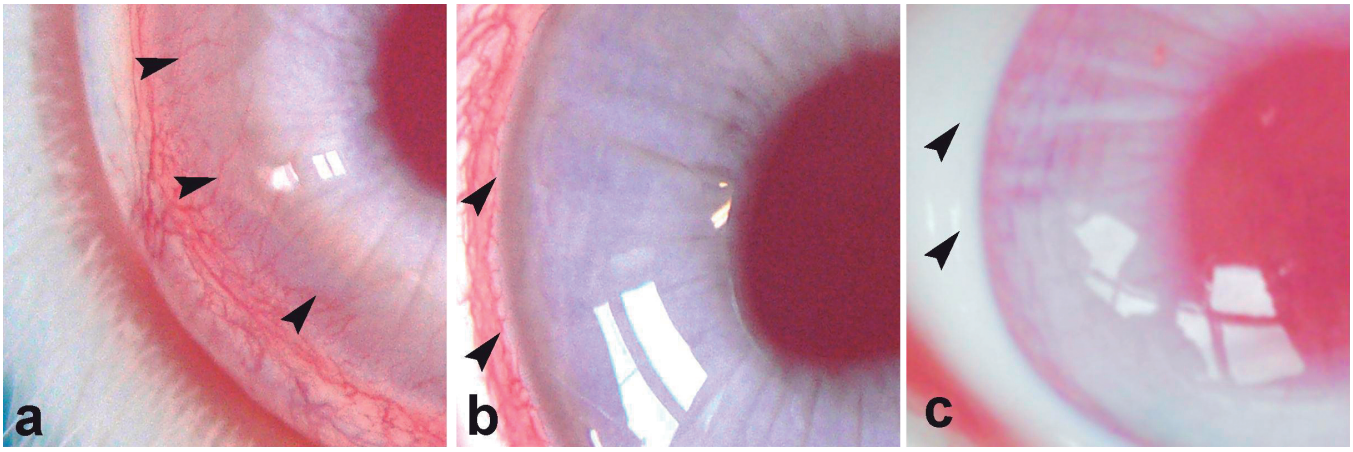

Fig. 7. Detail of corneal neovascularization (macroscopic images). **a.** Irradiated cornea treated with buffered saline for three weeks after irradiation. Corneal neovascularization (arrows) is apparent in the limbal region. **b.** Irradiated cornea treated with trehalose drops for three weeks after the end of irradiation. Corneal neovascularrization is suppressed. Perilimbal vessels are visible at the corneal-scleral transition (black arrows). **c.** Normal cornea (without any perilimbal vessels, arrows).

(Elbein et al., 2003; Chen and Haddad, 2004; Minutoli et al., 2007; Chen et al., 2009; Jain and Roy, 2009; Luyckx and Baudouin, 2011). Trehalose is not synthesized by mammalian cells; however, providing trehalose exogenously also enhanced the resistance of mammalian cells against a variety of environmental stresses. Thus, the utilization of trehalose for therapeutic purposes seems to be promising. In ophthalmology, trehalose has been used to protect cells of the anterior eye surface against dessication stress in dry eye disease (Matsuo, 2001; Matsuo et al. 2002; Chen et al. 2009; Luyckx and Baudouin, 2011). Takeuchi et al. (2010, 2011) suggested that trehalose has the potential for use as a new agent to control fibrosis – and is thus promising for use in glaucoma surgery. Trehalose was also found to be effective against oxidative stress of the cornea after UVB irradiation (Čejková et al., 2010, 2011). This is important because oxidative stress accompanies a number of human corneal diseases (Buddi et al., 2002).

The UVB-irradiated cornea is damaged by oxidative stress. Oxidative stress is caused by an imbalance between the production of reactive oxygen species and their removal. UVB radiation induces the generation of reactive oxygen species. Repeated irradiation of the rabbit cornea evoked a profound decrease in antioxidants, whereas prooxidants remained at normal levels or even increased (Čejková et al., 2000, 2004; Lodovici et al., 2003). This antioxidant/prooxidiant imbalance, together with the more pronounced production of nitric oxide generated by nitric oxide synthases, led to the formation of cytotoxic nitrogen-related oxidants, such as peroxynitrite, generated by the rapid reaction of nitric oxide with superoxide (Čejková et al., 2005).

However, the UVB-irradiated cornea is damaged not only by reactive oxygen species induced by UVB irradiation, but also by hypoxic-response injury, because damaged corneal cells cannot utilize oxygen normally, although the oxygen supply to the cornea is normal (Scheufler, 2004). This greatly contributes to delayed re-epithelialization, the ingrowth of vessels into the cornea and apoptotic cell death.

In our previous papers it was described that trehalose applied on the corneal surface during UVB irradiation effectively protected the cornea against oxidative damage (Čejková et al., 2010, 2011). In the UVB-irradiated cornea, trehalose decreased the antioxidant/prooxidant imbalance and apoptotic cell death, reduced proinflammatory cytokine and matrix metalloproteinase induction and greatly suppressed corneal neovascularization. Trehalose might act as a scavenger of oxyradicals. Toxic oxygen products have a damaging effect on amino acids in cellular proteins, and the presence of trehalose in cells prevents this damage (Elbein et al., 2003). Chen and Haddad (2004) described the efficacy of trehalose against hypoxic or anoxic injury. According to these authors, trehalose is an example of how this disaccharide molecule can enhance protein integrity and limit protein degradation not only in oxidant injury, but also in hypoxia or anoxia. Because until now no information existed about the possibility of using trehalose to inhibit hypoxic-response injury in the UVB injured cornea, we decided to study this problem in order to fill this gap.

The results of this study show the efficacy of trehalose in accelerating corneal healing. According to Rogers et al. (2004), sub-solar UVB radiation already causes irreversible damage to the corneal epithelium. Apoptosis appears to be a mechanism of corneal cell death after UVB ray exposure (Podskochy et al., 2000; Newkirk et al., 2007; Pauloin et al., 2009). Pauloin et al. (2009) showed that the exposure of human corneal epithelial cells to UVB rays leads to the activation of caspase-3, which serves as a critical marker of apoptosis. In our previous experiments with UVB-irradiated corneas in which trehalose was dropped on the corneal surface during irradiation, we found that trehalose greatly prevented the apoptotic death of corneal cells. The results of this study (when trehalose was applied on the cornea for one week following the end of repeated irradiation) show that apoptotic cell death was significantly reduced in the irradiated corneas. After two weeks of trehalose treatment, apoptopic cells were not observed in the cornea, whereas after buffered saline application apoptotic cell death was apparent in the cornea at the end of the second week of treatment (Fig. 1) (also at the end of the third week).

Very similar results were obtained with peroxynitrite formation, lipid peroxidation and urokinase type plasminogen activator expression. Although after the end of irradiation a high number of UVB-irradiated corneal epithelial cells was stained for these markers, following one week of trehalose treatment the number of positively stained corneal epithelial cells was reduced, and after two weeks of trehalose application positive staining was absent, or present in very low expression (urokinase type plasminogen activator). Staining was not present similarly as in the normal (untreated) corneal epithelium. The sections or samples on Millicell membranes were stained only with counterstaining (haematoxylin) (Figs. 2-4). In contrast, after buffered saline application, the number of positively stained corneal epithelial cells (for active caspase-3, nitrotyrosine, malondialdehyde and urokinase type plasminogen activator) was high in UVB irradiated corneas following two weeks of treatment after injury, and were also present in significant numbers at the end of the third week (Figs. 2-4, Table 1) .

The detection of peroxynitrite formation (immunohistochemically by nitrotyrosine residues), a toxic reaction product of nitric oxide and superoxide, serves as an important marker of free radical damage of ocular tissues. Allen et al. (1996, 1998) described that peroxynitrite caused oxidative damage of cell membranes in the eye and the formation of cytotoxic aldehydes. Elevated nitrotyrosine staining has been found in UVB-irradiated corneas (Čejková et al., 2005). Malondialdehyde staining is a good marker of lipid

peroxidation, which is an important biological consequence of the oxidative damage of cell membranes and the formation of cytotoxic aldehydes. These aldehydes can result in altered enzyme activities, the inhibition of DNA/RNA synthesis and other damaging events (Esterbauer et al., 1991). Urokinase-type plasminogen activator is a serine protease that converts plasminogen to plasmin and then activates pro-matrix metalloproteinases. It degrades the extracellular matrix, stimulates cell migration, proliferation and chemotaxis and induces angiogenesis (Chao et al., 2011). The appearance and possible role of urokinase-type plasminogen activator and plasmin has been described previously in the UVB-irradiated cornea (Čejková and Lojda, 1995).

Summarizing our results with the healing of corneas treated with trehalose or buffered saline, trehalose accelerated the healing of UVB-irradiated corneas. Compared to buffered saline application, after trehalose treatment corneal disorders, examined immunohistochemically and morphologically, recovered one to two weeks earlier than after buffered saline application. Similar results were obtained with the restoration of corneal transparency and the suppression of corneal neovascularization (Figs. 5-7).

In conclusion, the promoting effect of trehalose on corneal wound healing is likely to be related to a decrease in the hypoxia-response injury of the cornea. Trehalose inhibited apoptotic cell death, suppressed peroxynitrite formation and malondialdehyde staining and greatly reduced the overexpression of urokinase-type plasminogen activator. Because the results of immunohistochemical staining on cryostat sections corresponded with the results of similar staining on corneal impression cytologies, corneal impression cytologies, using suitable markers of injury, are a promising tool for diagnostic purposes.

Acknowledgements. Supported by a grant from the Academy of Sciences of the Czech Republic AVOZ50390512. We thank Laboratoires Thea for supplying the eye drops under study and Taras Ardan, MD for photographical documentation of experimental animals and technical support.

References

Allen J.B., McGahan M.C., Fleisher L.N. and Privalle C.T. (1996). Intravitreal lipopolysaccharide (LPS) induced peroxynitrite formation. Invest. Ophthalmol. Vis. Sci. 37, S918.

Allen J.B., Keng T. and Privalle C.T. (1998). Nitric oxide and peroxynitrite production in ocular inflammation. Environ. Health Perspect. 106, Suppl. 5, 1145-1149.

Buddi R., Lin B., Atilano S.R., Zorapapel N.C., Kenney M.C. and Brown D.J. (2002). Evidence of oxidative stress in human corneal diseases. J. Histochem. Cytochem. 50, 341-351.

Cejka C., Platenik J., Guryca V., Sirc J., Michalek J., Brunova B. and Čejková J. (2007). Light absorption properties of the rabbit cornea repeatedly irradiated with UVB rays. Photochem. Photobiol. 83, 652-657.

Čejková J. and Lojda Z. (1995). The appearance of active plasminogen activator of urokinase type (u-PA) in the rabbit anterior eye segment irradiated by UVB rays. A histochemical and biochemical study. Acta Histochem. 97, 257-262.

Čejková J., Stipek S., Crkovska J. and Ardan T. (2000). Changes of antioxidant enzymes in the cornea of albino rabbits irradiated with UVB rays. Histochemical and biochemical study. Histol. Histopathol. 15, 1043-1050.

Čejková J., Stipek S., Crkovska J., Ardan T., Platenik J., Cejka C. and Midelfart A. (2004). UV Rays, the prooxidant/antioxidant imbalance in the cornea and oxidative damage. Physiol. Res. 53, 1-10.

Čejková J., Ardan T., Cejka C., Kovaceva J. and Zidek Z. (2005). Irradiation of the rabbit cornea with UVB rays stimulates the expression of nitric oxide synthases-generated nitric oxide and the formation of cytotoxic nitrogen-related oxidants. Histol. Histopathol. 20, 467-473.

Čejková J., Ardan T., Simonová Z., Cejka C., Malec J., Dotrelová D. and Brunová B. (2008). Decreased expression of antioxidant enzymes in the conjunctival epithelium of dry eye (Sjögren's syndrome) and its possible contribution to the development of ocular surface oxidative injuries. Histol. Histopathol. 23, 1477-1483.

Čejková J., Cejka C., Ardan T., Sirc J., Michalek J. and Luyckx J. (2010). Reduced UVB-induced corneal damage caused by reactive oxygen and nitrogen species and decreased changes in corneal optics after trehalose treatment. Histol. Histopathol. 25, 1403-1416.

Čejková J., Ardan T., Cejka C. and Luyckx J. (2011). Favorable effects of trehalose on the development of UVB-mediated antioxidant/prooxidant imbalance in the corneal epithelium, proinflammatory cytokine and matrix metalloproteinase induction, and heat shock protein 70 expression. Graefes Arch. Clin. Exp. Ophthalmol. 249, 1185-1194.

Chao S.C., Hu D.N., Yang P.Y., Lin C.Y. and Yang S.F. (2011). Overexpression of urokinase-type plasminogen activator in pterygia and pterygium fibroblasts. Mol. Vis. 17, 23-31.

Chen Q. and Haddad G.G. (2004). Role of trehalose phosphate synthase and trehalose during hypoxia: from flies to mammals. J. Exp. Biol. 207, 3125-3129.

Chen W., Zhang X., Liu M., Zhang J., Ye Y, Lin Y., Luyckx J. and QU J. (2009). Trehalose protects against ocular surface disorders in experimental murine dry eye through suppression of apoptosis. Exp. Eye Res. 89, 311-318.

Elbein A.D., Pan Y.T, Pastuszak I. and Carroli D. (2003). New insights on trehalose: a multifunctional molecule. Glycobiology 13, 17R-27R.

Esterbauer H., Schaur R.J. and Zollner H. (1991). Chemistry and biochemistry of 4-hydroxynonenal, malondialdehyde and related aldehydes. Free Radic. Biol. Med. 11, 81-128.

Fris M., Tessem M.B., Čejková J. and Midelfart A. (2006). The effect of single and repeated UVB radiation on rabbit cornea. Graefes Arch. Clin. Exp. Ophthalmol. 244, 680-1687.

Haaskjold E., Olsen W.M., Bjerknes R. and Kravik K. (1993). Early cell kinetic effects of a single dose of narrow-banded ultraviolet B irradiation on the rat corneal epithelium. Photochem. Photobiol. 57, 663-666.

Jain N.K. and Roy I. (2009). Effect of trehalose on protein structure. Protein Sci. 18, 24-36.

Koliopoulus J.X. and Margaritis L.H. (1979). Response of the cornea to far ultraviolet light: an ultrastructural study. Ann. Ophthalmol. 11, 765-769.

Lodovici M., Raimondi L., Guglielmi F., Gemignani S. and Dolara P. (2003). Protection against ultraviolet B-induced oxidative DNA

damage in rabbit corneal-derived cells (SIRC) by 4-coumaric acid. Toxicology 184, 141-147.

Luyckx J. and Baudouin Ch. (2011). Trehalose: an intriguing dissacharide with potential for medical application in ophthalmology. Clin. Ophthalmol. 5, 577-581.

Matsuo T. (2001). Trehalose protects corneal epithelial cells from death by drying. Br. J. Ophthalmol. 85, 610-612.

Matsuo T., Tsuchida Y. and Morimoto N. (2002). Trehalose eye drops in the treatment of dry eye syndrome. Ophthalmology 109, 2024-2029.

Minutoli L., Altavilla D., Bitto A., Polito F., Bellocco E., Lagana G., Giuliani D., Fiumara T., Magazu S., Ruggeri P., Guarini S. and Squadrito F. (2007). The dissacharide trehalose inhibits proinflammatory phenotype activation in macrophages and prevents mortality in septic shock. Shock 27, 91-96.

Newkirk K.M., Chandler H.L., Parent A.E., Young D.C., Colitz C.M.H., Wilkie D.A. and Kusewitt D.F. (2007). Ultraviolet radiation-induced corneal degeneration in 129 mice. Toxicol. Pathol. 35, 817-824.

Pauloin T., Dutot M., Joly F., Warnet J.M. and Rat P. (2009). High molecular weight hyaluronan decreases UVB-induced apoptosis and inflammation in human epithelial corneal cells. Mol. Vision 15, 577-583.

Podskochy A., Gan L. and Fagerholm P. (2000). Apoptosis in UV-exposed rabbit corneas. Cornea 19:99-103.

Rogers C.S., Chan L.M., Sims Y.S., Byrd K.D., Hinton D.L. and Twining S.S. (2004). The effects of sub-solar levels of UV-A and UV-B on rabbit corneal and lens epithelial cells. Exp. Eye Res. 78, 1007-1014.

Sasaki (2009). H. Sun's UV rays more dangerous in snow than on the beach (Authorized interview given by Hiroshi Sasaki to Danielle Demetriou, Tokyo, for The Daily Telegraph); 09 December 2009. http://www.telegraph.co.uk/science/6766419/Suns-UV-rays

Scheufler K.M. (2004). Tissue oxygenation and capacity to deliver O_2 do the two go together? Transfus. Apher. Sci. 31, 45-54.

Takeuchi K., Nakazawa M., Ebina Y., Sato K., Metoki T., Miyagawa Y. and Ito T. (2010). Inhibitory effects of trehalose on fibroblast proliferation and implications for ocular surgery. Exp. Eye Res. 91, 567-577.

Takeuchi K., Nakazawa M. and Ebina Y. (2011). Effects of trehalose on VEGF-stimulated angiogenesis and myofibroblast proliferation. Implications for glaucoma filtration surgery. Invest. Ophthalmol. Vis. Sci. 52, 6987-6993.

Tessem M.B., Bathen T.F., Čejková J. and Midelfart A. (2005). Effect of UV-A and UV-B irradiation on the metabolic profile of aqueous humor in rabbits analyzed by 1H NMR spectroscopy. Invest. Ophthalmol. Vis. Sci. 46, 776-781.

Wenk J., Brenneisen P., Meewes C., Wlaschek M., Peters T., Blaudschun R., Ma W., Kuhr L., Schneider L. and Scharffetter-Kochanek K. (2001). UV-induced oxidative stress and photoaging. Curr. Proobl. Dermatol. 29, 83-94.

Zigman S. (1995). Environmental near-UV radiation and cataracts. Optom. Vis. Sci. 72, 899-901.

Accepted February 17, 2012